Mitigation of railway induced vibrations by using heavy masses next to the track

A. Dijckmans[1], P. Coulier[1], J. Jiang[2], M.G.R. Toward[2], D.J. Thompson[2], G. Degrande[1], G. Lombaert[1]

[1]KU Leuven, Department of Civil Engineering, Kasteelpark Arenberg 40, B-3001 Leuven, Belgium
[2]Inst. of Sound and Vibration Research, University of Southampton, Southampton, SO17 1BJ, UK
email: arne.dijckmans@bwk.kuleuven.be, pieter.coulier@bwk.kuleuven.be, j.jiang@soton.ac.uk, m.g.r.toward@soton.ac.uk,
djt@isvr.soton.ac.uk, geert.degrande@bwk.kuleuven.be, geert.lombaert@bwk.kuleuven.be

ABSTRACT: The effectiveness of heavy masses next to the track to reduce railway induced vibration is discussed. These heavy masses next to the track could be built as a gabion wall also used as noise barriers or as a concrete wall. Since the performance of mitigation measures on the transmission path is strongly determined by local ground conditions, a parametric study has been performed for a range of possible designs in a set of different ground types. A 2.5D coupled finite element - boundary element methodology was adopted, assuming that the geometry of the problem is invariant in the longitudinal direction along the track. It is found that the gabion walls start to be effective above a mass-spring resonance frequency which is determined by the mass of the gabion wall and the stiffness of the soil. A gabion wall will be more effective at sites with a soft soil. Increasing the mass will improve the insertion loss at lower frequencies. The effectiveness at higher frequencies is increased by making the footprint of the gabion walls as large and stiff as possible, and by placing the masses next to each other without any connection. For homogeneous soil conditions, the effectiveness is nearly independent of the distance behind the walls. When a softer top layer is present, the wave impeding effect is strongly decreased with increasing distance behind the walls.

KEY WORDS: ground-borne vibration, heavy masses, gabion wall, 2.5D, finite element, boundary element.

1 INTRODUCTION

Railway induced vibrations can be a source of annoyance for line-side residents. In case of excessive vibration levels, mitigation measures can be taken at the source, on the transmission path or at the building where vibration problems occur. Within the frame of the EU FP7 project 'Railway induced vibration abatement solutions (RIVAS)' [1], mitigation measures at the source and on the transmission path within the railway infrastructure have been studied for tracks at grade. This paper focuses on the application of heavy masses next to the track as a vibration mitigation measure on the transmission path. Up to now, very little research has been carried out about the practical use of masses on the ground surface to reduce railway induced vibrations, and hence little is known about its effectiveness.

Jones [2] and Krylov [3] studied the effect of individual masses such as concrete or stone blocks placed on the ground surface alongside the track. These irregularities at the surface cause a scattering of the incident surface waves into surface and body waves, resulting in a possible reduction of the wave field transmitted into the free field. The reduction is expected to be especially strong near the natural frequency of the oscillating mass on the soil [2,3]. In the case of a two-dimensional geometry, calculations indicate insertion loss values of up to 8-14 dB in a frequency range of about 40 % around the natural frequency [3]. Experimental tests with 600 kg concrete masses failed to give conclusive results [2].

Insight into the mitigation effect of heavy masses can also be gained from similar studies in other scientific domains, such as solid state physics [4]. Oscillators or irregularities at the surface of an elastic halfspace interacting with the surface

waves and causing wave scattering have been studied. The scattering turns out to be influenced by the spatial distribution and concentration of the oscillators. The interaction of buildings with the incident wave field has also been studied in the case of earthquakes [5-7]. It is shown that the wave field is reduced when the excitation frequencies are close to the building resonance frequencies, which can be the case for soft soils. It is also shown that a periodic structure of a city has little influence on the global scattering of waves [5].

In this paper, a continuous row of masses next to the track is considered, for example a gabion wall consisting of free-standing stackable wire-baskets filled with stones. Gabion walls have been installed as noise barriers next to railway lines (figure 1). In this case an acoustic nucleus is integrated within the wall to fulfill the acoustic requirements on noise absorption. Such a barrier could be designed as a combined barrier for airborne noise and ground-borne vibration.

Figure 1. A gabion wall installed as noise barrier next to a railway track (source: www.heringinternational.com).

2   METHODOLOGY

2.1   2.5D coupled FE-BE model

Within the frame of RIVAS, a theoretical parametric study has been carried out by project partners KU Leuven and ISVR for different mitigation measures on the transmission path, including trenches, barriers, subgrade stiffening and heavy masses [8,9]. Independent analysis was first conducted by both project partners for several benchmark cases.

In the study, the geometry of the track-soil system is assumed to be invariant in the longitudinal direction. This simplifying assumption enables the use of a computationally efficient two-and-a-half-dimensional (2.5D) approach, where the Fourier transform of the longitudinal coordinate allows to represent the three-dimensional (3D) response of the structure and the radiated wave field on a two-dimensional (2D) mesh.

At KU Leuven, the 2.5D approach has been followed to predict vibrations induced by road and railway traffic. For the computation of the dynamic interaction between a layered soil and structures with a longitudinally invariant geometry, a coupled finite element - boundary element (FE-BE) methodology formulated in the frequency domain is used [10]. The classical 2.5D FE method is combined with the 2.5D BE method using 2.5D Green's functions of a horizontally layered halfspace [11]. In this way, the free surface and the layer interfaces of the halfspace do not have to be discretized with boundary elements, avoiding spurious reflections at mesh truncations. The BE mesh can be limited to the interface between the structure and the soil, significantly reducing the size of the BE mesh.

The 2.5D coupled FE and BE model used at ISVR was originally developed by Nilsson and Jones [12] to investigate ground-structure vibration and airborne noise. It includes solid FE and BE, fluid FE and BE, as well as beam and plate structures. Fundamental solutions of a homogeneous full space are used for the boundary elements so the ground surface and any layer interfaces need to be carefully meshed to a sufficient distance. A special edge element is used to avoid the reflection at the end of ground or layer mesh.

Figure 2 schematically shows the problem considered in the parametric study of heavy masses next to the track. A continuous wall with height h and width w is placed on the soil at a distance R from the centre of the track. The geometry of the problem is assumed to be invariant in the longitudinal
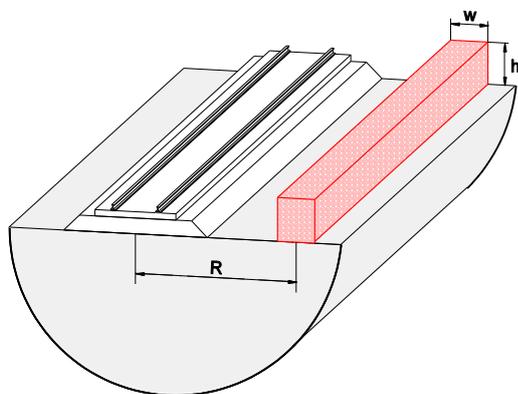
direction along the track. The main variables considered in the parametric study are the size and position of the wall, the dynamic properties of the wall, and the soil characteristics. The following sections give a description of the track, soil and mass properties used in the study.

2.2   Track properties and track model

The reference track used in the parametric study consists of UIC60 rails, supported by rail pads on monoblock concrete sleepers and a ballast layer with a height of 0.30 m. No sub-ballast, form layer or embankment is included. The parameters of the track are summarized in Table 1.

Table 1. Characteristics of the track

Part	Characteristic	Value	Dimension
Rail	Bending stiffness	6.4	[x10⁶ N/m²]
	Mass per unit length	60	[kg/m]
	Gauge	1.435	[m]
Rail pad	Stiffness	300	[x10⁶ N/m]
	Loss factor	0.10	[-]
Sleeper	Length	2.60	[m]
	Width	0.25	[m]
	Height	0.20	[m]
	Mass	325	[kg]
	Young's modulus	30	[x10⁹ N/m²]
	Poisson's ratio	0.15	[-]
	Sleeper distance	0.60	[m]
Ballast	Height	0.30	[m]
	Shear wave velocity	300	[m/s]
	Poisson's ratio	1/3	[-]
	Density	2000	[kg/m³]
	Material damping ratio	0.02	[m]
	Upper width	3.6	[m]
	Lower width	5.6	[m]

The model of the rails, the rail pads and the sleeper contains four degrees of freedom in the plane of the cross section (vertical motion and rotation of the sleeper and vertical motion of left and right rail). The rails are modelled as Euler-Bernoulli beams, the rail pads as continuous spring-damper connections and the sleepers as a uniformly distributed mass, rigid in the plane of the cross section. The ballast is modelled as an elastic continuum by means of eight-node quadrilateral 2.5D finite elements.

2.3   Soil properties

The parametric study is focused on three reference sites: Horstwalde, Lincent and Furet. The dynamic soil characteristics (layer thickness h, shear wave velocity C_s, dilatational wave velocity C_p, density ρ, and material damping ratios β_s and β_p in both deviatoric and volumetric deformation) for the three sites are given in Table 2, Table 3 and Table 4. The site at Horstwalde is a homogeneous halfspace. The site of Lincent consists of two softer top layers above a relatively

Figure 2. Geometry of the 2.5D model for heavy masses next to a railway track

Table 2. Soil characteristics for the Horstwalde site.

Layer	h [m]	C_s [m/s]	C_p [m/s]	β_s [-]	β_p [-]	ρ [kg/m³]
1	∞	250	1470	0.025	0.025	1945

Table 3. Soil characteristics for the Lincent site.

Layer	h [m]	C_s [m/s]	C_p [m/s]	β_s [-]	β_p [-]	ρ [kg/m³]
1	1.4	128	286	0.044	0.044	1800
2	2.7	176	286	0.038	0.038	1800
3	∞	355	1667	0.037	0.037	1800

Table 4. Soil characteristics for the Furet site.

Layer	h [m]	C_s [m/s]	C_p [m/s]	β_s [-]	β_p [-]	ρ [kg/m³]
1	2	154	375	0.025	0.025	1800
2	10	119	290	0.025	0.025	1850
3	∞	200	490	0.025	0.025	1710

stiff halfspace. At the site of Furet, an inverse layering is present and the second, softest layer goes down to a depth of 12 m.

2.4 Dynamic properties of heavy masses

The properties of the heavy masses next to the track used in the parametric study are based on the properties of gabion walls. Gabions used as noise barriers usually have a width of 1 m and a height of 0.5 m or 1 m. The length of the gabions can vary between 1 m and 5 m. Several of these gabions can be combined to increase the width and height of the barrier.

An overview of the material parameters (density ρ, shear wave velocity C_s, Poisson's ratio v, and material damping ratio β) used in the parametric study for the gabion walls can be found in Table 5. To investigate the influence of the dynamic properties of the wall, a concrete wall next to the track has also been considered. The material properties used for the concrete wall are listed in Table 5.

Table 5. Dynamic properties of gabion and concrete wall.

	ρ [kg/m³]	C_s [m/s]	v [-]	β [-]
Gabions	1700	300	0.20	0.02
Concrete	2400	2280	0.20	0.0

3 NUMERICAL RESULTS

3.1 Benchmark reference case

The case of a gabion wall with a height $h = 2$ m and a width $w = 1$ m placed at the Horstwalde site at $R = 4$ m from the track centreline, which is the typical distance of noise barriers, is taken as the reference. This reference case was also used as a benchmark for the 2.5D models developed at ISVR and KU Leuven. To facilitate the interpretation of the results, the track has been disregarded in the reference case. The wall was modelled as an elastic continuum by means of 2.5D finite elements taking into account the flexibility of the cross section and wave propagation in the longitudinal direction. Figure 3 shows the transfer mobilities between a vertical point load applied at the soil and the vertical displacement at a distance of 24 m for the cases with and without gabion wall. The corresponding insertion loss values are shown in Figure 4. The gabion wall has no effect on the wave propagation at frequencies below 30 Hz, apart from a small peak in insertion loss at 12 Hz. Around 60 Hz, a peak value of 8 dB is visible in the insertion loss curve. Above this frequency, the insertion
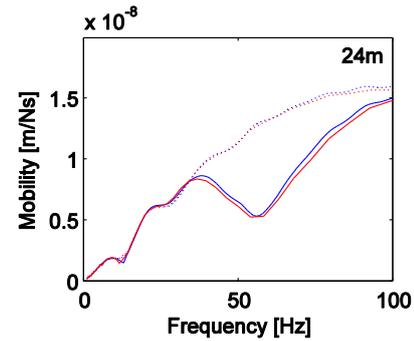

Figure 3. Transfer mobility at a distance of 24 m for a gabion wall (width 1 m, height 2 m) at the Horstwalde site. Cases with (solid lines) and without (dotted lines) gabion wall. KU Leuven results (blue), ISVR results (red).
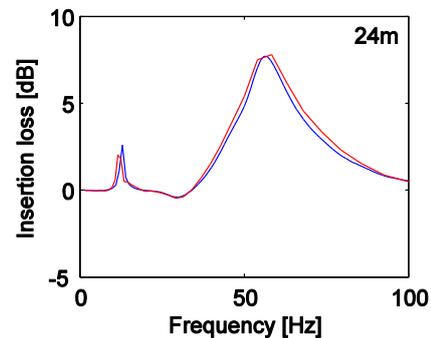

Figure 4. Vertical insertion loss at a distance of 24 m for a gabion wall (width 1 m, height 2 m) at the Horstwalde site. KU Leuven results (blue), ISVR results (red).

loss starts to decrease again. Results of the KU Leuven model are compared with results of the ISVR model, showing a very good agreement between both models.

3.2 Physical mechanisms

In order to investigate the underlying physical mechanisms, additional simulations have been performed for the reference case without track. Simplified models have been used for the gabion wall to enable physical interpretation. First, the gabion wall is modelled as a distributed line mass on the soil with a footprint of 0.01 m. Second, a rigid cross section for the gabion wall is considered, only allowing for a global vertical translation and rotation of the wall cross section. The stiffness in the longitudinal direction is neglected in both models.

Figure 5 compares the insertion loss at a receiver distance of 24 m for both simplified models. The insertion loss at the soil-mass interface is also shown for a 2D calculation. The behaviour of the distributed line mass resembles that of a mass-spring system. At low frequencies, the mass follows the vertical displacement at the soil's surface and no reduction is seen. Around the mass-spring resonance frequency of 31 Hz, a clear dip is observed in the insertion loss at the soil-mass interface. Above the resonance frequency, the insertion loss rises steeply due to the inertia of the mass. The mass-spring resonance frequency f_0 can be estimated from [3]:

$$f_0 = \frac{1}{2\pi}\sqrt{\frac{K_s}{m}} \qquad (1)$$

where m is the total mass of the gabion wall per unit length
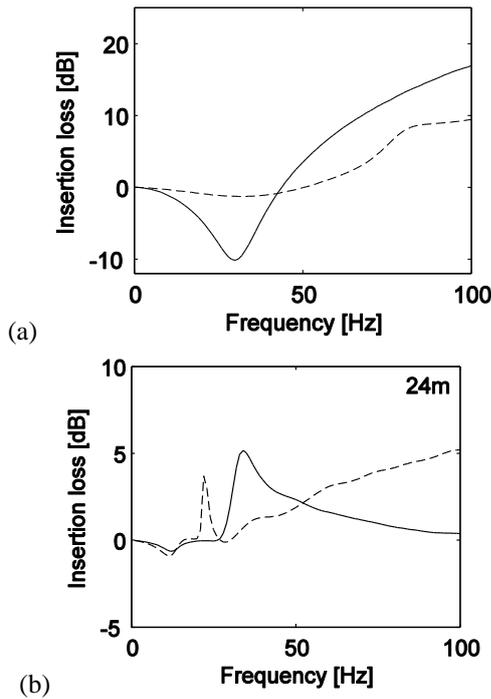
(a)

(b)

Figure 5. Influence of footprint on insertion loss at (a) the soil-mass interface for a 2D case and (b) a receiver distance of 24 m for a vertical point load applied at the soil (3D case). A gabion wall modelled as a distributed line mass without stiffness in longitudinal direction (solid lines) and modelled with a rigid cross section without stiffness in longitudinal direction (dashed lines).
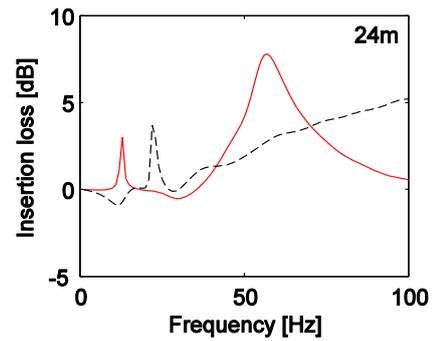

Figure 6. Influence of cross section flexibility on insertion loss at a receiver distance of 24 m for a point load applied at the soil. A gabion wall (width 1 m, height 2 m) modelled with rigid (black dashed line) and flexible (red solid line) cross section without stiffness in longitudinal direction.
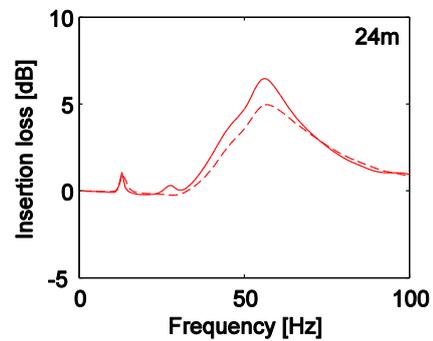

Figure 7. Influence of longitudinal stiffness on insertion loss at a receiver distance of 24 m for a line load applied at the soil. A gabion wall (width 1 m, height 2 m) modelled with flexible cross section without stiffness in longitudinal direction (solid line), and modelled with flexible cross section with stiffness in longitudinal direction (dashed line).

and K_s represents the stiffness of the soil under the mass per unit length. An estimation for K_s can be found from the vertical soil stiffness for a rigid strip foundation.

Still considering the case of a distributed line mass, the insertion loss at 24 m starts to increase at the mass-spring resonance frequency of 31 Hz. This leads to a maximum in the insertion loss curve at 35 Hz. While the insertion loss at the soil-mass interface reaches very high values at higher frequencies, the insertion loss behind the distributed line mass starts to decrease again above 35 Hz. Only a small reduction is seen above 50 Hz.

When the gabion wall is modelled as a wall with footprint 1.0 m and rigid cross section, the mass-spring resonance dip in the insertion loss at the soil-mass interface is less clear (figure 5a). The resonance frequency is slightly shifted to a higher frequency compared to that of the distributed line mass. From this resonance frequency on, the insertion loss at 24 m increases steadily with increasing frequency (figure 5b). In contrast to the results for the distributed line mass, a large reduction is also obtained at higher frequencies for positions behind the gabion wall. In this frequency range, the rigid mass will block the wave field along the interface. A small peak in the insertion loss curve can be seen at 22 Hz. This peak is related to a rocking mode of the gabion wall and therefore not observed when the wall is modelled as a distributed line mass.

When the flexibility of the cross section of the gabion wall is taken into account, the behaviour of the gabion wall is significantly changed, especially at frequencies above 40 Hz (figure 6 which compares the results for figures 4 and 5).

In this frequency range, the width of the wall is of the same order of magnitude as the Rayleigh wavelength. The interaction between the Rayleigh waves and the wall will depend strongly on the flexibility of the gabion wall and its footprint. Above the mass-spring resonance dip around 30 Hz, the insertion loss increases strongly up till a frequency of 60 Hz. The frequency at which the gabion wall starts to reduce vibrations behind the wall corresponds to the mass-spring resonance frequency. This cut-on frequency is the same as for the wall with rigid cross section. The frequency range in which a considerable reduction is obtained is broader compared to the case of the distributed line mass. The insertion loss value is however considerably lower at higher frequencies than for the wall with a rigid cross section. These results indicate that it is beneficial to make the footprint of the gabion walls as large and stiff as possible.

The influence of the stiffness in the longitudinal direction has also been investigated as it is not clear what stiffness is provided by the gabions in practice. Figure 7 shows the insertion loss at a receiver distance of 24 m for a line load. The line load consists of 16 uncorrelated unit vertical point forces applied at the soil at the axle positions of a four-car EMU train. The longitudinal stiffness has a small effect on the insertion loss for a line load. In the frequency range between 40 Hz and 60 Hz, the insertion loss is 1 dB lower when the

longitudinal stiffness is taken into account. This indicates that it is better to place the masses next to each other without any connection.

In the following sections, the influence of soil conditions, receiver position, size, position and dynamic properties of the gabion wall on the one-third octave band insertion loss values for a line load is investigated. The track has been included in these calculations. A flexible cross section has been assumed for the gabion walls and wave propagation in the longitudinal direction has been taken into account.

3.3   Influence of soil conditions

The influence of the layering of the soil on the effectiveness of the 2 m high and 1 m wide gabion wall is investigated in this section. When the soil properties vary with depth, the propagation of Rayleigh waves is dispersive. The existence of multiple modes with different cut-on frequencies makes the interaction of the gabion wall with the soil more complex.

Figure 8 compares the one-third octave band insertion loss values of the gabion wall at 8 m at the three reference sites. For the site of Horstwalde, the insertion loss is negligible up to a frequency of 30 Hz. Above the mass-spring resonance frequency, the insertion loss increases up to a maximum value of approximately 5 dB at 63 Hz. At higher frequencies, the insertion loss starts to decrease again due to the flexibility of the wall. Due to the softer soil at Furet, the mass-spring resonance frequency is lower and the gabion wall starts to reduce vibrations from 8 Hz on with a large reduction above 63 Hz. For the site of Lincent, two maxima are visible in the insertion loss curve. The first maximum occurs in the frequency range 20-30 Hz. A second peak value is seen in the frequency band of 63 Hz. Below 20 Hz and above 63 Hz, the reduction is negligible.
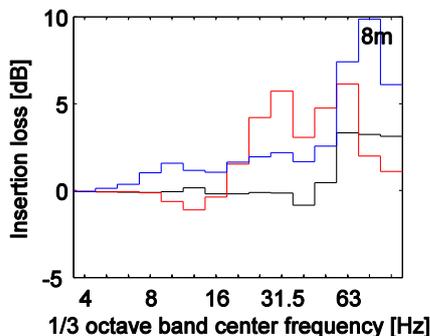

Figure 8. Influence of the soil conditions on the effectiveness of a gabion wall (width 1 m, height 2 m). Vertical insertion loss for a line load at a distance of 8 m for the Horstwalde site (black), the Lincent site (red) and the Furet site (blue).

3.4   Influence of receiver distance and depth

Figure 9 shows the spatial dependence of the insertion loss for a 1 m wide and 2 m high gabion wall installed at the Horstwalde site in the case a harmonic point force is applied to the rails with an excitation frequency of 30 Hz, 60 Hz and 90 Hz. At 30 Hz, the wave field is not affected by the presence of the gabion wall, leading to an insertion loss of zero almost everywhere in the soil domain. At 60 Hz, the
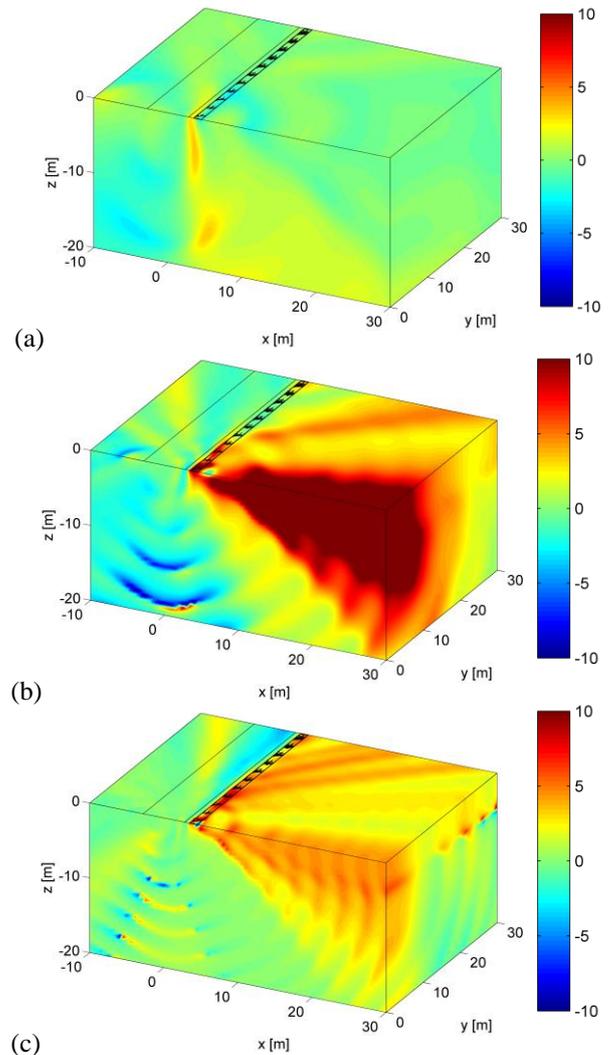

Figure 9. Insertion loss (in dB) of a gabion wall (width 1 m, height 2 m) at the Horstwalde site for a point load applied to the track at a frequency of (a) 30 Hz, (b) 60 Hz and (c) 90 Hz.

gabion wall can effectively reduce the vibration levels. A reduction of more than 10 dB is obtained in the central zone around the line perpendicular to the track at the position where the load is applied. Overall, the insertion loss decreases with increasing angle from this line. The insertion loss at 90 Hz is lower than at 60 Hz, but more uniformly distributed along the surface behind the gabion wall. Both at 60 Hz and 90 Hz, no overall increase in vibration levels is observed at the opposite side of the track.

Figure 10 shows the influence of the receiver distance on the one-third octave band insertion loss values at the three reference sites. Four receiver distances at the surface are considered: 8 m, 16 m, 32 m and 64 m. For the site of Horstwalde, the insertion loss is almost independent of the receiver distance. At 8 m, the reduction is smaller between 40 Hz and 63 Hz. Around the mass-spring resonance frequency of 40 Hz, there is even an increase in vibration levels. At Lincent, the insertion loss decreases strongly with increasing distance behind the wall. At 8 m, a dip in insertion loss is seen around the mass-spring resonance frequency of 12 Hz. The effectiveness of the gabion wall decreases for

(a)

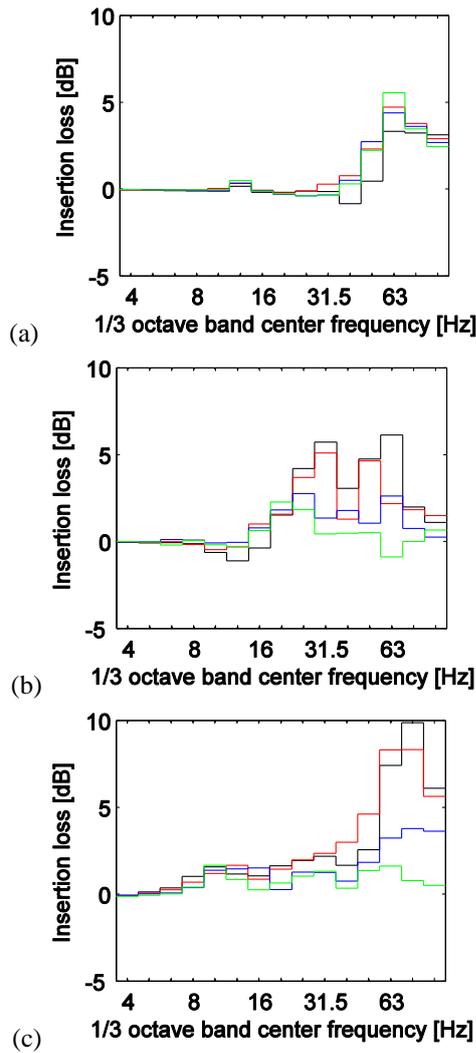(b)

(c)

(a)

(b)

(c)

Figure 10. Influence of the receiver distance on the vertical insertion loss for a line load of a gabion wall (width 1 m, height 2 m) at (a) the Horstwalde site, (b) the Lincent site and (c) the Furet site. Receiver distance 8 m (black), 16 m (red), 32 m (blue) and 64 m (green) from the track.
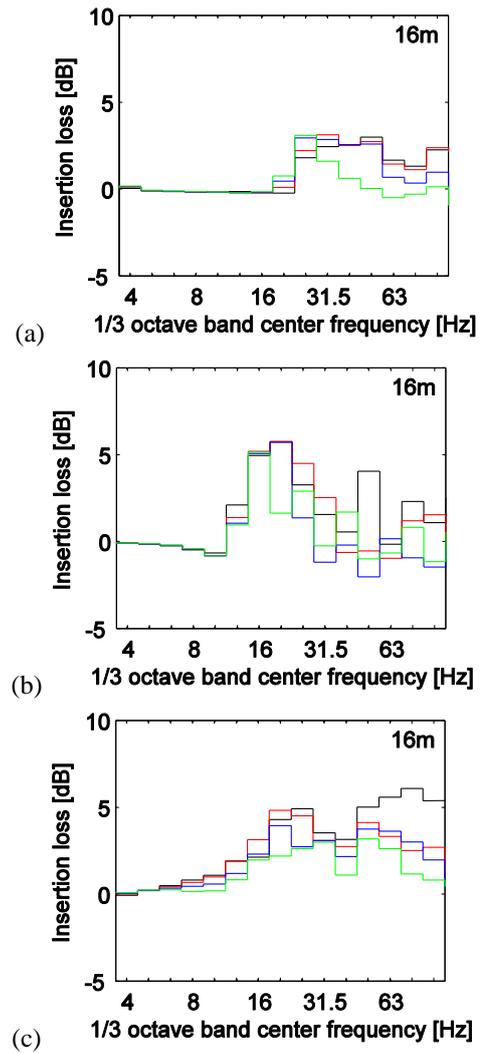
Figure 11. Influence of the receiver depth on the vertical insertion loss at 16 m for a line load of a gabion wall (width 1 m, height 2 m) at (a) the Horstwalde site, (b) the Lincent site and (c) the Furet site. Receiver depth 0 m (black), 3 m (red), 6 m (blue) and 9 m (green).

larger distances behind the wall for the site of Furet as well, especially at higher frequencies.

Figure 11 shows the influence of the receiver depth at the three reference sites. The vertical insertion loss at a receiver distance of 16 m is shown for four receiver depths: 0 m, 3 m, 6 m and 9 m. As can be expected, the influence of receiver depth is negligible at low frequencies and becomes more apparent at high frequencies for all three reference sites. For Horstwalde, the reduction is significant down to a depth of 6 m. At the site of Furet, the insertion loss decreases gradually with increasing depth. For Lincent, the receiver depth of 3 m is located in the middle of the second layer, while the receiver points at a depth of 6 m and 9 m are located in the stiffer halfspace (Table 3). The reduction at frequencies above 30 Hz is limited in the halfspace.

3.5 Influence of height of gabion wall

In this section, the influence of the height of the gabion wall is investigated. Three heights are considered: 2 m, 4 m and 6 m.

Figure 12a shows results for the Horstwalde site. Increasing the height of the gabion wall improves the effectiveness at low frequencies. The mass-spring resonance frequency which determines the onset of vibration reduction is decreased by increasing the mass of the wall. For the 2 m high wall, the insertion loss starts to increase in the frequency band of 40 Hz. For the 4 m and 6 m high walls, the increase starts in the frequency bands of 20 Hz and 16 Hz, respectively. The peak value in insertion loss is also shifted towards a lower frequency by increasing the height of the wall. The same trends are visible in the results for Lincent (figure 12b). If the height of the wall is increased from 2 m to 4 m, the peak value in insertion loss is shifted from 25 Hz to 16 Hz. Increasing the height of the gabion wall to 6 m will further improve the efficiency at low frequencies, with a maximum reduction of 5 dB at 12.5 Hz. Above 20 Hz, the influence of the height of the wall is limited. For the site of Furet, increasing the height does not lead to a consistent improvement in performance at
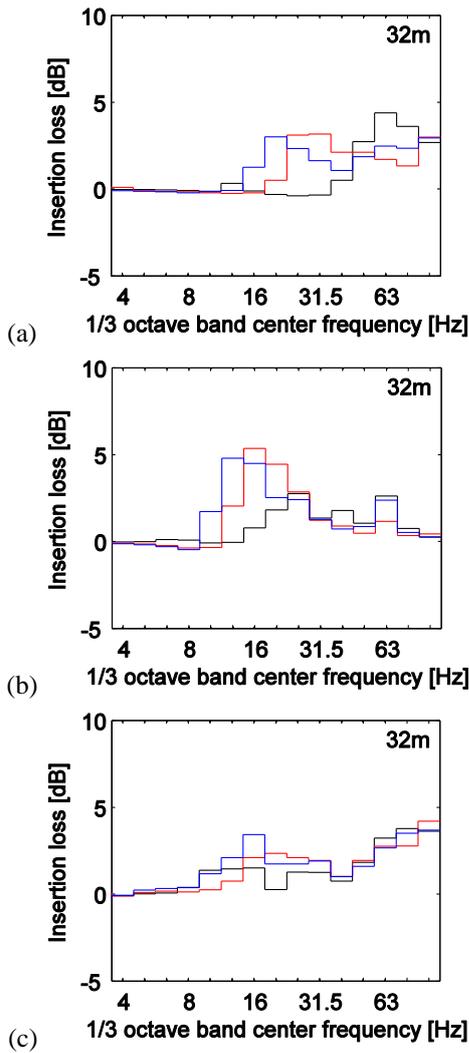
(a)

(b)

(c)

Figure 12. Influence of the height of a 1 m wide gabion wall at (a) the Horstwalde site, (b) the Lincent site and (c) the Furet site. Vertical insertion loss for a line load at a receiver distance of 32 m for a height of 2 m (black), 4 m (red) and 6 m (blue).
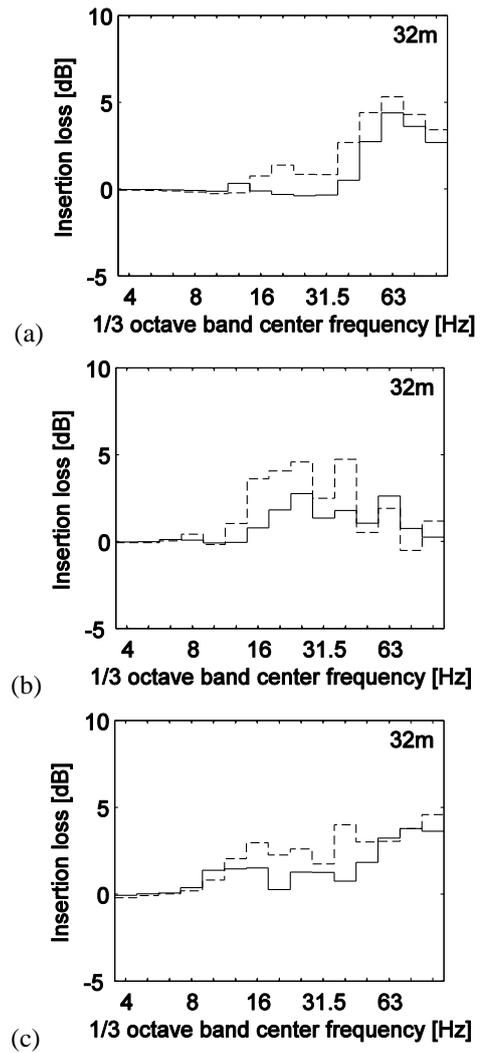

(a)

(b)

(c)

Figure 13. Influence of the width of a 2 m high gabion wall at (a) the Horstwalde site, (b) the Lincent site and (c) the Furet site. Vertical insertion loss for a line load at a receiver distance of 32 m for a width of 1 m (solid lines) and 2 m (dashed lines).

low frequencies (figure 12c). Again, the height has little influence at higher frequencies.

3.6 Influence of width of gabion wall

Figure 13 shows the influence of the width of a gabion wall with a height of 2 m at the reference sites of Horstwalde, Lincent and Furet. The width is set to 1.0 m and 2.0 m. For all three sites, doubling the width of the wall increases the effectiveness in a broad frequency range. The higher mass results in a lower mass-spring resonance frequency and therefore an improved performance at low frequencies. Furthermore, Rayleigh waves can be blocked more effectively due to the larger footprint. As a result, the insertion loss is also improved at higher frequencies.

3.7 Influence of position of gabion wall

When a gabion wall is used as a noise barrier, it is usually placed as close to the track as possible. Here, the influence of the position of the gabion wall next to the track is investigated

by doubling the distance from the track. Figure 14 shows the insertion loss at 32 m for a line load at the Horstwalde site. The peak value in insertion loss at 63 Hz is decreased by 1 dB by doubling the distance. Also at higher frequencies, a small decrease in insertion loss is seen.

3.8 Influence of dynamic properties of masses

Finally, the influence of the dynamic properties of the heavy masses next to the track is investigated by comparing the effectiveness of a gabion wall with the effectiveness of a continuous concrete wall at the Horstwalde site. The material properties used for the concrete wall are given in Table 5. Both walls have a height of 2 m and a width of 1 m and are placed at a distance of 4 m from the centre of the track. Figure 15 shows the insertion loss at a distance of 32 m from the track for a line load. For the gabion wall, the insertion loss starts to increase above 35 Hz and a peak value in insertion loss is visible in the frequency band of 63 Hz. For the concrete wall, the increase in insertion loss starts at lower frequencies.
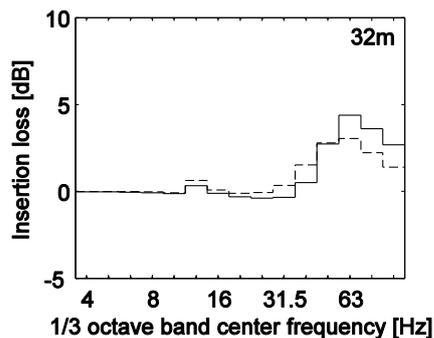
Figure 14. Influence of the position of a gabion wall (width 1 m, height 2 m) at the Horstwalde site. Vertical insertion loss for a line load at a distance of 32 m for a gabion wall at 4 m (solid line) and 8 m (dashed line) from the centre of the track.
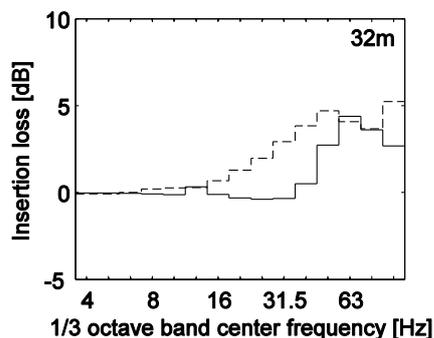

Figure 15. Comparison between a gabion wall (solid line) and a concrete wall (dashed line) with height 2 m and width 1 m. Vertical insertion loss at 32 m for a line load at the Horstwalde site.

This improvement at low frequencies cannot be explained by the increase in mass only, but is largely the result of the increased stiffness of the wall. Further calculations (not shown here for brevity) have shown that the concrete wall at the surface acts as a stiff wave barrier when the contrast in stiffness between the soil and the wall next to the track is sufficiently large. Longitudinal bending waves excited in the wall will cause a large reduction of vibration above a critical frequency in an area determined by a critical angle [8].

4 CONCLUSION

In this paper, a row of heavy masses next to the track consisting of gabions has been studied by means of 2.5D simulations. The gabion walls can give a reduction in vibration levels above a mass-spring resonance frequency which is determined by the mass of the gabion wall and the stiffness of the soil. A 2 m high and 1 m wide gabion wall is effective above 40 Hz at the Horstwalde site. By doubling the height of the wall, this cut-on frequency is lowered to 20 Hz. The lower the stiffness of the soil, the lower the mass-spring resonance frequency. Therefore, a gabion wall will be more effective at sites with a soft soil. For the site of Lincent, the mass-spring resonance frequency equals 12 Hz for a 2 m high and 1 m wide gabion wall resulting in a reduction of vibration levels above 16 Hz. For the site of Furet, this gabion wall starts to reduce vibration from 8 Hz on. At frequencies above the mass-spring resonance frequency, Rayleigh waves are

hindered due to the blocking of the wave field by the masses along the interface. It is therefore important to make the footprint of the gabion walls as large and stiff as possible. Furthermore, calculation results indicate that it is better to place the masses next to each other without any connection. On the other hand, if the contrast between the stiffness of the soil and the longitudinal stiffness of the wall next to the track is large enough, a continuous wall can act as a stiff wave barrier. Calculations should be complemented with measurements to determine the actual behaviour of the gabion walls and investigate the validity of the assumptions made in the parametric study.

REFERENCES

[1] http://www.rivas-project.eu
[2] C.J.C. Jones. Use of numerical models to determine the effectiveness of anti-vibration systems for railways. *Proceedings of the Institution of Civil Engineers-Transport*, 105(1):43-51, 1994.
[3] V.V. Krylov. Scattering of Rayleigh waves by heavy masses as method of protection against traffic-induced ground vibrations. In H. Takemiya, editor, *Environmental vibrations. Prediction, Monitoring, Mitigation and Evaluation*, pages 393-398. Taylor and Francis Group, London, 2005.
[4] E.A. Garova, A.A. Maradudin, and A.P. Mayer. Interaction of Rayleigh waves with randomly distributed oscillators on the surface. *Physical Review B*, 59(20):13291-13296, 1999.
[5] D. Clouteau and D. Aubry. Modification of the ground motion in dense urban areas. *Journal of Computational Acoustics*, 9(4):1659-1675, 2001.
[6] G. Lombaert and D. Clouteau. The resonant multiple wave scattering in the seismic response of a city. *Waves in Random and Complex Media*, 16(3):205-230, 2006.
[7] G. Lombaert and D. Clouteau. Elastodynamic wave scattering by finite-sized resonant scatterers at the surface of a horizontally layered halfspace. *Journal of the Acoustical Society of America*, 125(4):2041-2052, 2009.
[8] P. Coulier, A. Dijckmans, J. Jiang, D.J. Thompson, G. Degrande, and G. Lombaert. Stiff wave barriers for the mitigation of railway induced vibrations. *Proceedings of the 11th International Workshop on Railway Noise IWRN11*, pages 599-606, Uddevalla, Sweden, September 2013.
[9] J. Jiang, M.G.R. Toward, A. Dijckmans, D.J. Thompson, G. Degrande, G. Lombaert, and J. Ryue. Reducing railway induced ground-borne vibration by using trenches and buried soft barriers. *Proceedings of the 11th International Workshop on Railway Noise IWRN11*, pages 615-622, Uddevalla, Sweden, September 2013.
[10] S. François, M. Schevenels, G. Lombaert, P. Galvín, and G. Degrande. A 2.5D coupled FE-BE methodology for the dynamic interaction between longitudinally invariant structures and a layered halfspace. *Computer Methods in Applied Mechanics and Engineering*, 199(23-24):1536-1548, 2010.
[11] M. Schevenels, S. François, and G. Degrande. EDT: An ElastoDynamics Toolbox for MATLAB. *Computers & Geosciences*, 35(8):1752-1754, 2009.
[12] C.-M. Nilsson and C.J.C. Jones. Theory manual for WANDS 2.1. ISVR Technical Memorandum 975, University of Southampton, 2007.